# AN INVESTIGATION OF THE EFFECT OF FEEDBACK CONTROL ON THE BIFURCATION STABILITY OF A NONLINEAR SERVOHYDRAULIC SYSTEM

**Amit Shukla[1] and David F. Thompson[2]**

[1]*Department of Mechanical and Manufacturing Engineering, Miami University, Oxford, Ohio 45056, USA*
[2]*Department of Mechanical, Industrial and Nuclear Engineering, University of Cincinnati, Ohio 45221, USA*
*shuklaa@muohio.edu, david.thompson@uc.edu*

**Abstract**

The Servo-hydraulic systems are commonly used for motion and force control and exhibit nonlinear dynamic phenomena. One such nonlinear phenomenon is the loss of stability via bifurcations. In this work, a computational and experimental investigation is performed to characterize with a higher degree of accuracy the effect of linear feedback control on the bifurcation stability of a nonlinear servo-hydraulic system. A low-order model of the experimental test stand is first developed, validated and analyzed. It is then shown that the use of an appropriate linear feedback control structure can improve the bifurcation stability of a nonlinear servo-hydraulic system. Parametric space investigation is conducted to study the bifurcation stability behavior of the system and stability boundaries are developed to demonstrate the effect of linear feedback on the nonlinear systems.

**Keywords:** Servo-hydraulic, bifurcation, feedback control, nonlinear system

## 1 Introduction

Design of servo-hydraulic systems is a challenge because of the ever-increasing demands on the performance and economics of the intended systems. Further, these systems have been optimized in design over so many years that further improvement is harder to achieve using the linear system theory. Current practice places stringent demands on these systems by requiring these systems to be more reliable and robust in a larger design space.

The servo-hydraulic systems also provide for interesting dynamical behavior due to the presence of the square root flow nonlinearity and coupling between the hydraulic and mechanical response. Also, these systems have complex dynamics associated with them due to the presence of friction, hard limits, complicated port flows, and intricate coupling between various components in the circuit. A typical servo-hydraulic circuit (Kremer and Thompson, 1998) consists of servo valves, orifices, tubes, volumes, pumps, solenoid valves, etc. They exhibit modes, which range from very slow (drift) to very fast ones (McCloy and Martin, 1980) (as associated with the valve spool and flapper dynamics).

This manuscript was received on 20 November 2003 and was accepted after revision for publication on 15 April 2005

Nonlinear systems such as servo-hydraulic systems can undergo loss of stability due to change in system parameters. When qualitative change in the dynamics occurs due to a small change in a system parameter it is broadly classified as a *bifurcation*. Such phenomena usually manifest themselves in the form of fluid pressure and flow oscillations (with accompanying vibration of mechanical elements). In some settings, this behavior is also classified as a *self-excited* oscillation. The emergence of bifurcations is equivalent to loss of stability of an equilibrium condition in nonlinear systems. Various types of bifurcations exist and have been investigated by various researchers including Jordan and Smith (1999). A numerical investigation of the bifurcation stability on a servo-hydraulic system was conducted by Shukla and Thompson (2001, 2002). Some experimental studies on the stability of servo-hydraulic systems were also conducted by Kowta (2003).

This ever increasing demand on the performance and stability of these systems can be fulfilled by the use of appropriate feedback control structures. The two primary goals of this work are 1) to study bifurcation stability behavior of a specific servo-hydraulic system by developing stability boundaries in parametric space and 2) to study the effect of linear controllers on bifurcation stability of this system. Specifically, the aim is to demonstrate that for linear controllers, increased controller order can be effective in modifying the bifurcation stability behavior of a nonlinear servo-hydraulic system. In this work a servo-valve actuator system is developed as a hydraulic system test stand (Fig. 1). A reduced-order model of this test stand is also developed and validated. The bifurcation stability behavior due to parametric variation of this test-stand system for a non zero flow operating condition is predicted. These results are also experimentally verified.

Thus, the main goal of this work is to conduct nonlinear parametric bifurcation stability analysis for a servo-valve actuator system. Further, the effect of a baseline PD controller and a ninth–order linear controller is studied on the bifurcation stability of the servo-valve actuator system. The essential contributions of this research are to:

1. Demonstrate the effect of control on the bifurcation stability of a servo-hydraulic system. It is shown in this work that it is possible to extend the bifurcation stability boundary in the parameter space by suitable design of a linear feedback control law.
2. Demonstrate the value of bifurcation analysis in characterization of the overall nonlinear stability properties of such systems.

The role of experimental test stand is to verify the bifurcation stability result as predicted by the computational analysis.

## 2 Experimental Test Stand Development

The experimental apparatus is developed in conjunction with the *Parker Hannifin Hydraulic Trainer* (Fig. 1) which is a low-pressure device developed specifically for industrial and university training in fluid power applications. Due to equipment and cost constraints associated with this project, the trainer is used for its hydraulic power supply as well as for the servo-valve and its associated manifold. The cylinder test stand (Fig. 1) consists of a reaction stand for supporting an electro-hydraulic cylinder (Krutz, 2001). The electro-hydraulic cylinder used in this test stand is made by Parker Hannifin Corporation (model number 3LXLTS34A7). These cylinders are equipped with *MTS Temposonics* linear differential transducer (LDT) (model number LHTRB00U00701V0) to measure cylinder position. The servo-valve used for this analysis is a flapper-nozzle type servo-proportional valve (Merritt, 1967) made by Parker Hannifin Corporation (model number DY05AFCNA5). The hydraulic power supply consists of the gear pump installed on the Parker Trainer. To reduce the effect of pump noise in the supply pressure, a diaphragm type accumulator (charged to 2.76 MPa) is used with a supply pressure of 3.10 MPa. As stated in the introduction to this Section, this relatively low value of supply pressure is used as an academic demonstration and is not intended to replicate any specific application of servo-hydraulic system. However, the hydraulic circuit itself is commonly found in various applications including aircraft hydraulic control systems. This is appropriate for the goal of this study, which is to conduct parametric bifurcation stability analysis.

A pair of 2 m (approx. 6 ft) flexible hoses were used as a pipeline connecting the hydraulic servo-valve to the actuator. Such an arrangement is generally undesirable in most practical applications, due to the potential of transmission line modes; however, since the goal of this study is to characterize fundamental dynamics and stability behavior, this does not pose a specific performance limitation as long as the dynamics are modeled with appropriate accuracy. Additionally, accumulators (charged to a nominal value of 1.035 MPa) are introduced into the circuit as described further in Section 3; the specific goal of this is to make the system amenable for control studies by enabling adjustment of system natural frequencies (i.e., to within available control bandwidth) through reduction of the effective system bulk modulus.

A high-pressure inline filter is used to guarantee the cleanliness of the hydraulic fluid. The servo-valve current driver card (Parker BD101-24) is controlled by a *Matlab* based real time data acquisition and control hardware and software (*WINCON 3.2*), developed by *Quanser Consulting* (www.quanser.com). The pressure signal is measured by means of PCB Piezotronics static pressure sensor (model number 1502A02FJ1 KPSIS).

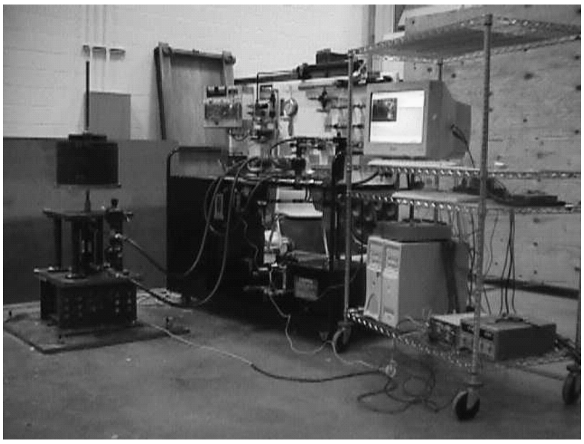

**Fig. 1:** *Servo-hydraulic test stand with real-time control hardware*

The servo-valve consists of a flapper-nozzle stage and a cylindrical spool stage. The details of operation and construction of a typical flapper nozzle servo-valve are discussed by several authors including Merritt (1967). Generally, the nonlinearities in this valve can be due to the nonlinear torque motor, flapper dynamics, nonlinear flow through nozzles, nonlinear flow forces on flapper, pressure-flow dynamics, spool dynamics, clearance in feedback spring and nonlinear port flow in the spool. These nonlinearities are inherent to the system and their interaction can lead to highly nonlinear dynamic behavior of the overall test-stand. The dynamics, control and stability of servo-hydraulic systems have been studied in detail by numerous investigators some of which include Alleyne and Liu (1999), Burton (1975) Blackburn, Reethof and Shearer (1960), Cox and French (1986), Foster and Kulkarni (1968), Fuerst, Hahn and Hecker (1997), Kremer and Thomson (1998), Lewis and Stern (1962), Maccari (2000), McCloy and Matrin (1980), Scheidl and Manhartsgruber (1998), Van Schothorst (1997), Viersma (1980), Watton (1988) and Yau, Bajaj, and Nwokah (1992). The primary aim of this work is to demonstrate a method for accurately characterizing the effect of linear feedback control structures on the bifurcation stability of a servo-hydraulic system via experimentation as well as numerical computation.

## 3 Reduced-Order Model Development

A flapper-nozzle servo-valve can be modeled by first principles (Merritt, 1967), but preliminary simulation studies showed that flapper dynamics had no significant effect on the system dynamics below 800 Hz. Thus, a reduced-order model of the servo-valve is developed. This reduction is based on the physics of the system and is developed iteratively based on experimental data. The aim is to approximate the full nonlinear dynamic characteristics of the servo-valve by decomposing it in two parts (Fig. 2). Based on the simulation studies, it was decided that the two parts consist of a linear transfer function from command voltage ($V(s)$) given to the valve amplifier card to the spool position ($X(s)$) of the valve and a nonlinear pressure-flow-voltage static (*i.e.*, algebraic) characteristic of the form $q = q(x_{valve}, \Delta p)$, where $q$ is the flow through the valve for a valve position input of $x_{\text{valve}}$ and pressure differential $\Delta p$.

The servo-valve has a flow throughput based on the command voltage and the pressure differential across the servo-valve. This is referred to as pressure-flow-voltage characteristics. In order to capture the nonlinear nature of the pressure-flow-voltage characteristics of the servo-valve, several static tests were conducted. These static tests involved studying response of the servo-valve for a dummy load (needle valve). The data obtained is shown in Fig. 4. Customarily, valve flow is modeled as a sharp edged orifice with an appropriate laminar to turbulent transition and depends on the pressure differential across the valve and the valve opening (Merritt 1967). Further, it was experimentally observed that the flow constant for the valve is also a function of the command voltage applied to the valve. Based on experimental data, the valve flow, $q$ (gal/min) characteristics can be modeled as in Eq. 1:

$$q = k_{\text{valve}}(V)\sqrt{|\Delta p|}\,sign(\Delta p) \qquad (1)$$

where $V$ is the valve input voltage, $k_{\text{valve}}(V)$ is a function of valve discharge coefficient, hydraulic fluid density, nominal valve spool diameter and valve spool position. This approach is similar to previous studies in which the variable discharge coefficient of the servo-valve based on the valve position was used (Viall and Zhang, 2000).

The valve is symmetrical and has no measurable dead-band. After experimental investigations (Fig. 3), the following fifth-order polynomial model for the effective $k_{\text{valve}}$ is developed as given in Eq. 2. The effect of pressure differential (Fig. 3) is captured by Eq. 1.

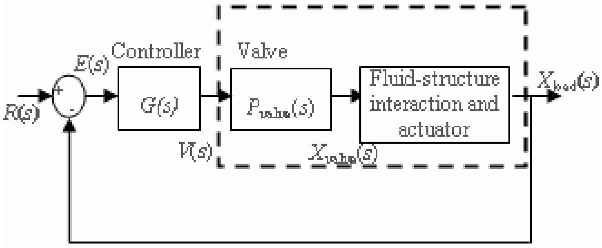


**Fig. 2a:** *Nonlinear model decomposition of test stand*

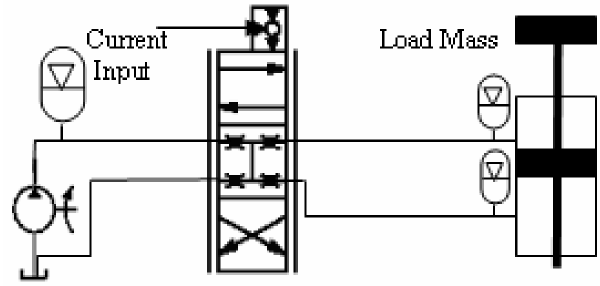


**Fig. 2b:** *Servo-valve actuator system- open loop schematic*

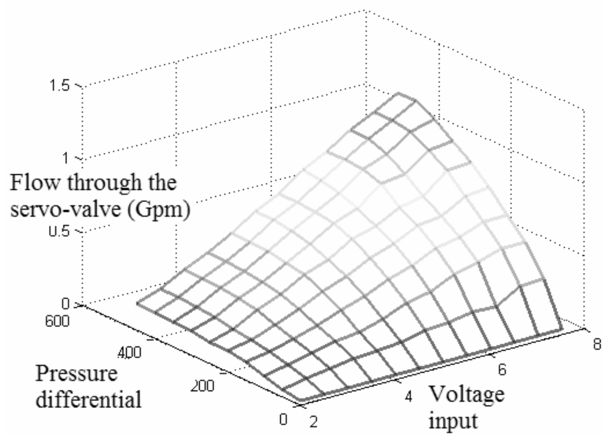


**Fig. 3:** *Pressure-differential-voltage input–flow throughput characteristics of the servo-valve*

$$\begin{aligned} k_{\text{valve}}(V) &= a_5V^5 + a_4V^4 + a_3V^3 + .... \\ &\quad a_2V^2 + a_1V^1 + a_0 \\ a_0 &= 0 \quad a_1 = 2.984E-3 \\ a_2 &= 4.827E-4 \; a_3 = 9.829E-5 \\ a_4 &= -1.264E-5 \quad a_5 = 3.852E-7 \end{aligned} \qquad (2)$$

The linear transfer function (voltage input to spool position output) representation of the valve is given in Eq. 3:

$$X(s) = \frac{k}{(1+\frac{s}{2\pi 80})^2(1+\frac{s}{2\pi 900})}V(s) \qquad (3)$$

where $k$ is 0.005 in/V. The servo-valve (Parker DYO5AFCNA5) does not have a measurable spool position output signal, so an experiment was designed with a dummy orifice load to validate the transfer function. No other dynamics are observed in the range of 0-60 Hz. At higher frequencies, the signal to noise ratio is very low.

The line dynamics is the leading cause of limiting the system bandwidth in this case since the servo-valve is mounted at a distance from the hydraulic cylinder. As indicated in the introduction to Section 2, this particular experimental configuration was incorporated to utilize existing hardware, provide portability and reduce the cost of the overall experiment. Further, due to the distance between the servo-valve and the hydraulic cylinder, line dynamics plays an important role in the overall stability behavior of the test stand. It is essential to generate the loss of bifurcation stability to investigate the effect of various controllers on the system. To analyze this, the system needs to include appropriate dynamic models of the transmission lines. Theoretical models of a single transmission line carrying compressible fluid assume that the wall of the transmission line is rigid, flow through the line is laminar, temperature is constant, and flow is one-dimensional. Various investigators have studied line dynamics and their effects on servo-hydraulic systems including Viersma (1980) and Watton (1988). The modal approximation (Yang and Tobler, 1991) for the transmission line between valve and actuator is given in Eq. 4:

$$\begin{bmatrix}\dot{p}_{\mathrm{bi}}\\ \dot{Q}_{\mathrm{ai}}\end{bmatrix}=\begin{bmatrix}0 & (-1)^{i+1}Z_{\mathrm{o}}\lambda_{\mathrm{ci}}\\ \dfrac{-(-1)^{i+1}\lambda_{\mathrm{ci}}}{Z_{\mathrm{o}}\alpha^{2}} & \dfrac{-8\beta}{\alpha}\end{bmatrix}\begin{bmatrix}p_{\mathrm{bi}}\\ Q_{\mathrm{ai}}\end{bmatrix}+\ldots$$
$$\begin{bmatrix}0 & \dfrac{-2Z_{\mathrm{o}}}{D_{\mathrm{n}}}\\ \dfrac{2}{Z_{\mathrm{o}}D_{\mathrm{n}}\alpha^{2}} & 0\end{bmatrix}\begin{bmatrix}p_{\mathrm{a}}\\ Q_{\mathrm{b}}\end{bmatrix} \qquad (4)$$

where Eq. 4 represents the state space realization and $p_{\mathrm{a}}$ and $Q_{\mathrm{a}}$ denote pressure and flow at the inlet of the pipeline. $p_{\mathrm{b}}$ and $Q_{\mathrm{b}}$ denotes the pressure and flow at the outlet of the pipeline. The subscript $i$ in the pressure and flow states denote the contribution of the $i^{\mathrm{th}}$ mode related to that state. Also, the dissipation parameter, $D_{\mathrm{n}}$ and line impedance constant $Z_{\mathrm{o}}$ are given in Eq. 5. Also, the values of natural frequency modification factor ($\alpha$), and damping modification factor ($\beta$) are given in Table 1. All other parameters are associated with the hydraulic oil (Mobil DTE 24) and a 3/8 in. diameter pipeline is used.

$$D_{\mathrm{n}} = \frac{l\nu}{c_{\mathrm{o}}r^{2}} \qquad Z_{\mathrm{o}} = \frac{\rho_{\mathrm{o}}c_{\mathrm{o}}}{A_{\mathrm{o}}}$$
$$\lambda_{\mathrm{ci}} = \pi(i-0.5)/D_{\mathrm{n}} \quad i=1,2,3.. \qquad (5)$$

where $c_{\mathrm{o}}=\sqrt{\beta_{\mathrm{e}}/\rho_{\mathrm{o}}}$ and $A_{\mathrm{o}}=\pi r^{2}$. Also, $\beta_{\mathrm{e}}$ is the effective bulk modulus, $l$ is the line length, $\nu$ is kinematic viscosity, and $\rho_{\mathrm{o}}$ is the density. The effective bulk modulus (air free) is experimentally determined to be 480.5 MPa by Kowta (2003). The mass balance of the actuator chamber results in the state equations Eq. 6 of the actuator pressure for both sides of the actuator. This neglects (Eq. 6) the effect of external leakage.

$$\dot{P}_{\mathrm{a}} = \frac{\beta_{\mathrm{e}}}{A_{\mathrm{cylinder\_a}}x}(q_{\mathrm{a}}-q_{\mathrm{l}}-A_{\mathrm{cylinder\_a}}\dot{x})$$
$$\dot{P}_{\mathrm{b}} = \frac{\beta_{\mathrm{e}}}{A_{\mathrm{cylinder\_b}}x}(-q_{\mathrm{b}}+q_{\mathrm{l}}+A_{\mathrm{cylinder\_b}}\dot{x}) \qquad (6)$$

where $\dot{P}_{\mathrm{a}}$ and $\dot{P}_{\mathrm{b}}$ are the rate of change of pressure in the two chambers of actuator, $q_{\mathrm{l}}$ is the laminar leakage flow across the cylinder piston, $q_{\mathrm{a}}$ and $q_{\mathrm{b}}$ are the flow to the actuator chambers, $A_{\mathrm{cylinder\_a}}$ and $A_{\mathrm{cylinder\_b}}$ are the areas of the cylinder piston. The difference in the value of areas is due to actuation rod. The effect of the accumulators in the transmission line between the servo-valve and the actuator is assumed to be accurately reflected by the reduction of the effective bulk-modulus of the system $\beta_{\mathrm{e}}$. Hence the total effective bulk modulus of the system under study is given by Eq. 7:

$$\frac{1}{\beta_{\mathrm{eff\_w\_accu}}} = \frac{1}{\beta_{\mathrm{air\_free}}}+\frac{\%air}{1.4(P_{\mathrm{cylinder}}+P_{\mathrm{atm}})}+\ldots$$
$$\frac{1}{1.4(P_{\mathrm{accu\_charge}}+P_{\mathrm{atm}})} \qquad (7)$$

The model for the electro-hydraulic cylinder has two states associated with the cylinder position ($x$) and two states associated with the chamber pressures ($p$) (Scheidl and Manhartsgruber, 1998). The equation of motion describing the cylinder dynamics is as shown in Eq. 8:

$$m_{\mathrm{load}}\ddot{x}+c_{\mathrm{load}}\dot{x}+k_{\mathrm{load}}x$$
$$= P_{\mathrm{a}}A_{\mathrm{cylinder\_a}}-P_{\mathrm{b}}A_{\mathrm{cylinder\_b}} \qquad (8)$$

The overall nonlinear model of the system includes a position and a velocity state for the cylinder/actuator (based on Eq. 8), a valve position state (based on Eq. 3), a four state (two pressure and two flow states) approximation of each pipeline (based on Eq. 4), and two pressure states for the cylinder (Eq. 6), It should be noted that the total number of the states and the overall transfer function will depend on the number of modes utilized to approximate the pipeline dynamics.

**Table 1:** Natural frequency ($\alpha$) and damping modification factor ($\beta$) for the two-mode approximation of pipe line dynamics

| Mode # | $\alpha$ | $\beta$ |
|---|---|---|
| 1 | 1.06 | 2.31 |
| 2 | 1.05 | 3.38 |

The servo-valve actuator model schematic is given in Fig. 2(b). The closed loop transfer function of the servo-valve actuator system (using a nominal PD controller) as observed experimentally using a sine wave analysis is given in Fig.4. The frequency response of the differential equation model shows two modes (8Hz and 25.5 Hz). These two modes are also visible in the experimental observation and hence provide a reasonable degree of validation of the developed model. Apparently, the 8 Hz mode is related to the dynamics associated with the load mass and its interaction with the hydraulic fluid stiffness of the cylinder. The 25.5 Hz mode can be correlated to the first pipeline mode in the system model which includes the effect of accumulators. The dynamic behavior of the servo-valve actuator model developed in this study matches well with the experimental observations except for difference in the numerical and experimental damping values of the second mode (Fig. 4). This model is studied for bifurcation behavior in closed loop using two different control structures. These studies are discussed in the following section.

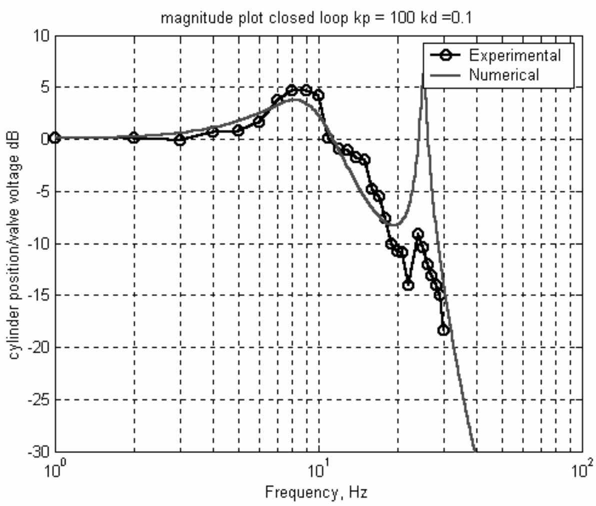


**Fig. 4:** *Experimental transfer function of the closed loop (PD controlled) servo-valve actuator system*

## 4 Control Studies

Two types of controllers are investigated; a PD (proportional plus derivative) controller and a ninth-order linear controller are used in this study for their effect on the bifurcation stability behavior of the servo-valve actuator system. All of the studies are conducted with the feedback of cylinder position signal measured by the LVDT. The effect of control on the bifurcation stability (Jordan and Smith, 1999) of the system is studied *under a constant velocity condition* (Shukla and Thompson, 2001, 2002). If operation is such that it is on a trajectory or flow where the cylinder is moving at a constant velocity then it is defined as a constant velocity solution. The advantage of analysis at a point on the trajectory other than zero velocity solution is in the excitation of the significant nonlinear response of the system (*i.e.*, zero input corresponds to the zero flow/zero velocity condition). The motivation for these control studies is to investigate the effect of controllers on the bifurcation stability behavior of the servo-hydraulic system. This comparison of stability characteristics would help characterize and design controllers for robust stability for nonlinear systems.

The general expectation is that a higher-order linear controller, when properly designed, would enhance the stability behavior of the nonlinear servo-hydraulic system as compared to the PD controller. This conclusion is well-known for linear plants, but nonlinear analysis is required to demonstrate a corresponding trend for nonlinear systems. Moreover, it should be noted that any such trend will be noted in specific cases and that general conclusions cannot be drawn. The work will characterize this improvement in stability behavior in parametric space by experimental as well as numerical observations.

A PD controller is very frequently used in industrial control systems. This is a logical first step in analyzing the effect of feedback on the system stability. The effect of PD control is to add a zero to the open loop system; from a linear feedback stability standpoint, the benefits of an appropriately placed zero are obvious. (As a practical matter, such a controller must also contain at least one pole which may be at high frequency; as such, ideal PD control must normally be approximated.) The zero of the controller may be placed using a model-based analysis, but it is also possible to employ a non-model-based approach in which the controller is tuned online.

The qualitative of change in the stability property of the equilibrium point as a parameter is moved is known as a *bifurcation*. This specific behavior of the loss of stability leading to a limit cycle oscillation is known as a *Hopf bifurcation*. The Hopf bifurcation occurs when a pair of complex eigenvalues crosses the imaginary axis as a parameter is moved, provided that some other technical conditions hold (Jordan and Smith, 1999; Guckenheimer and Holmes, 1983; Seydel, 1994; Strogatz, 2000). Further, if a system goes from an asymptotically stable equilibrium to a limit cycle as the parameter is increased through the critical value indicates that the system exhibits a *super-critical* Hopf bifurcation.

The results presented next in Fig. 5-7 and Fig. 8-11 indicate the effect of a varying parameter on the bifurcation stability of the overall system by tracking the change in the eigenvalues of the system via bifurcation analysis. This can be considered to be analogous to the root-locus plot for linear systems; in a traditional linear system root locus plot, the closed loop system poles (eigenvalues) are traced as a function of a system parameter, normally the open loop gain constant. However, in this case, bifurcation analysis provides additional insight by taking into account the parametric dependence of the equilibrium point, upon which the system Jacobian is dependent. In the eigenlocus plots shown (Fig. 5-7 and Fig. 8-11), the x-axis represents the real part and y-axis represents the imaginary part of the eigenvalues. The parameter(s) under study is highlighted in the caption of each figure and the result summarized by the identification of the critical frequency of Hopf bifurcation. The effect of increasing proportional gain in this system (Fig. 5) is to result in a Hopf bifurcation with critical frequency of 14.8 Hz which is depicted by the complex conjugate eigenvalue crossing the imaginary axis. The effect of increasing derivative gain is to result in the loss of stability of the transmission line dynamics mode as shown in Fig. 6. Variation of parameters on a two-dimensional grid of load mass and proportional gain is shown in Fig. 7. The effect of increase in the load mass is to decrease the critical bifurcation frequency of the system. The effect of increase in proportional gain is to result in Hopf bifurcation.

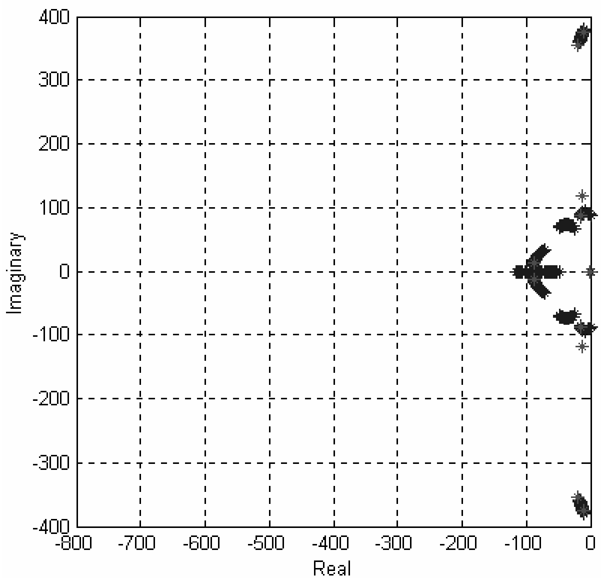


**Fig. 5:** *The effect of variation of proportional gain. Hopf bifurcation occurs at $K_p$=150, $K_d$=1 –PD controller with a critical frequency of 14.8 Hz*

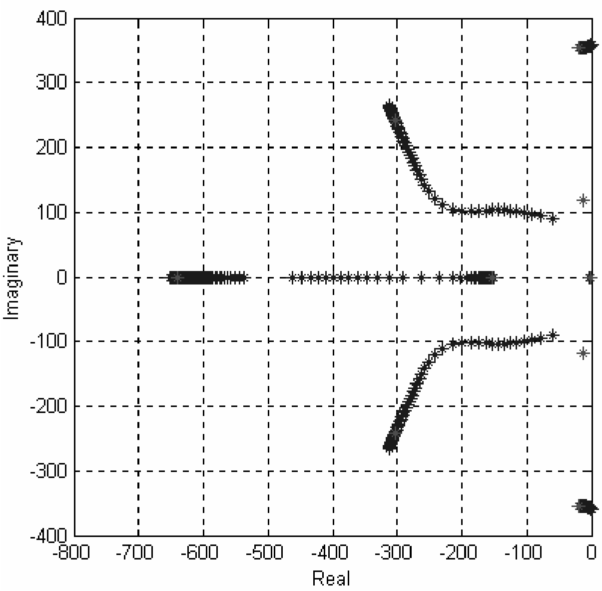


**Fig. 6:** *The effect of variation of derivative gain. Hopf bifurcation occurs at $K_p$=100, $K_d$=63 – PD controller with a critical frequency of 55.73 Hz*

The study of the PD controller showed that some control of the bifurcation stability behavior is possible by a simple feedback structure. A higher order (ninth-order) controller for a non-linear plant model based upon an operating condition of a 2 volt (10% of full scale) command input to the servo-valve with a load mass of 45.36 kg (100 lbs) and a supply pressure of 3.10 MPa (450 Psi) is designed with the general expectation that it would improve the stability of the servo-valve actuator system. As indicated in the introduction to Section 2, the two identical accumulators used to reduce the effective bulk modulus of the system, in order to facilitate this study, are charged at 1.035 MPa. System parameters including load mass and line pressure are selected to demonstrate the loss of stability via bifurcations.

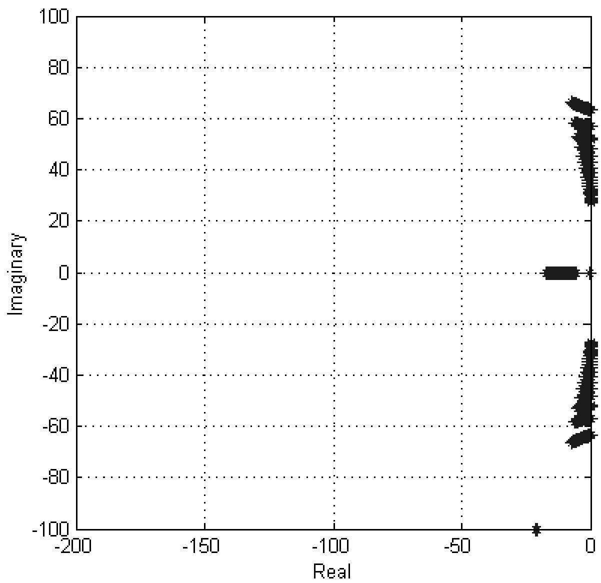


**Fig. 7:** *Effect of parameter variation on a grid of parameters ($K_p$, M)- PD controller. Critical frequency value ranges between 5 Hz and 11 Hz depending on the value of the load mass*

The compensator design was based on a nominal plant under the operating conditions outlined above. The performance specifications were selected based on a preliminary review of the uncompensated open loop Bode magnitude and phase plots. These plots were developed using a swept-sine wave simulation experiment (under the aforementioned operating conditions) using the reduced-order differential equation model outlined in Section 3. Based upon this review, it was decided that, with a modest amount of controller effort (i.e., in terms of controller frequency response magnitude), that a compensated system with at least $30^o$ phase margin and a gain margin of 3 db or more could realistically be achieved with an open loop bandwidth of 8 Hz, the latter figure being roughly equivalent to that of the nominal PD-compensated system. Towards these goals, a compensator was designed to shape the open loop Bode magnitude and phase plots so as to meet the assumed performance specifications. First, two pairs of complex conjugate zeros were added to cancel the nominal plant poles (around 8 Hz and 29 Hz). In addition to this, several poles were added to cut-off the high frequency response, which is generally necessary to reduce amplification of measurement noise entering in the feedback path (D'Azzo and Houpis, 1966). The higher-order control structure provides greater flexibility in the design of the controller. Using the frequency response shaping approach described, a controller consisting of four complex poles and zeros and an additional five poles is developed, resulting in a ninth-order compensator (Eq. 9). The open loop Bode gain and phase plot of the controller is shown in Fig. 8.

$$G(s)=\frac{\begin{array}{l}(1.43\text{E}15\ s^4+1.054\text{E}17\ s^3+\ldots\\ 5.39\text{E}19\ s^2+.2.39\text{E}21\ s+1.44\text{E}23)\end{array}}{\begin{array}{l}(s^9+5615\ s^8+1.042\text{E}7\ s^7+\ldots\\ 9.84\text{E}9\ s^6+5.84\text{E}12\ s^5+\ldots\\ 1.91\text{E}15\ s^4+4.22\text{E}17\ s^3+\ldots\\ 5.75\text{E}19\ s^2+4.4\text{E}21\ s+1.44\text{E}23)\end{array}} \quad (9)$$

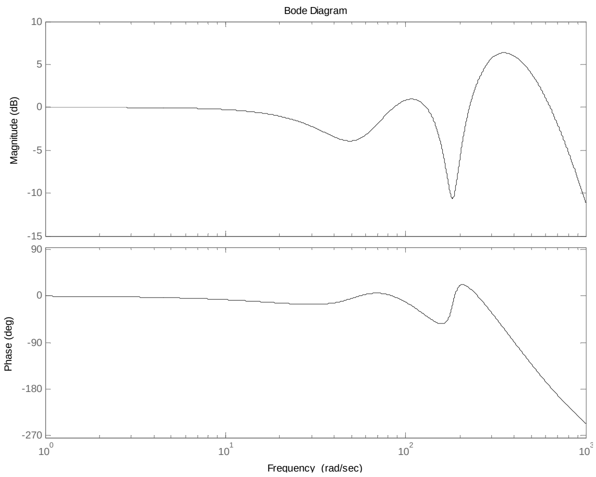


**Fig. 8:** *The Bode gain and phase plots for the $9^{th}$ order controller*

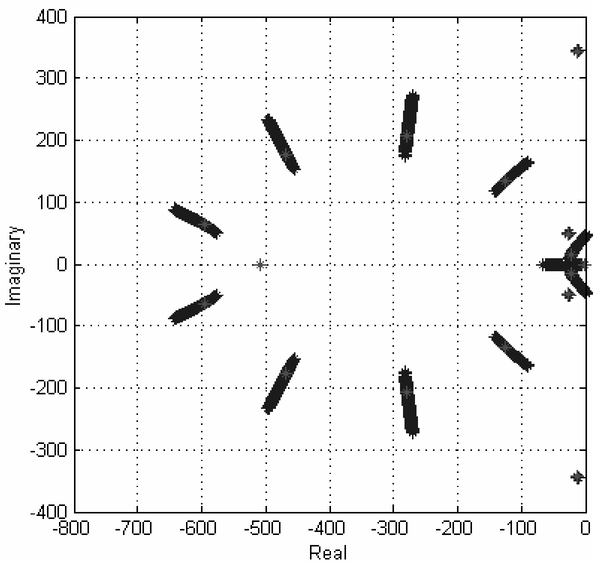


**Fig. 9:** *Effect of varying Bode gain of the controller ($K_v$). Hopf Bifurcation occurs at $K_v$=220, M=100 lb, V=0.2 in/sec-$9^{th}$ order controller with critical frequency of 8.75 Hz*

The effect of increasing the Bode (DC) gain of the ninth-order controller is to result in Hopf bifurcation with the critical frequency of 12 Hz (Fig. 9). The effect of increasing load mass is to result in a Hopf bifurcation with significantly lower critical frequency (Fig. 10). The effect of variation of parameters on the two dimensional space of the compensator Bode gain and the load mass is shown in Fig. 11.

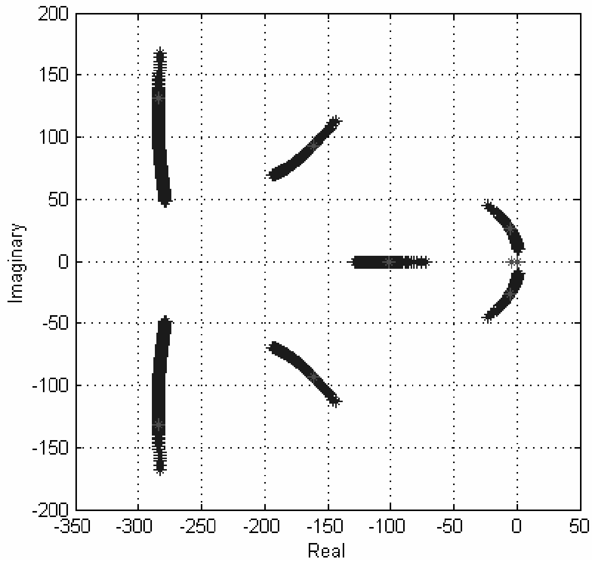


**Fig. 10:** *Effect of varying load mass. Hopf Bifurcation occurs at $K_v$=100, M=600 lb, V=0.2 in/sec.-$9^{th}$ order controller with critical frequency of 5.75 Hz*

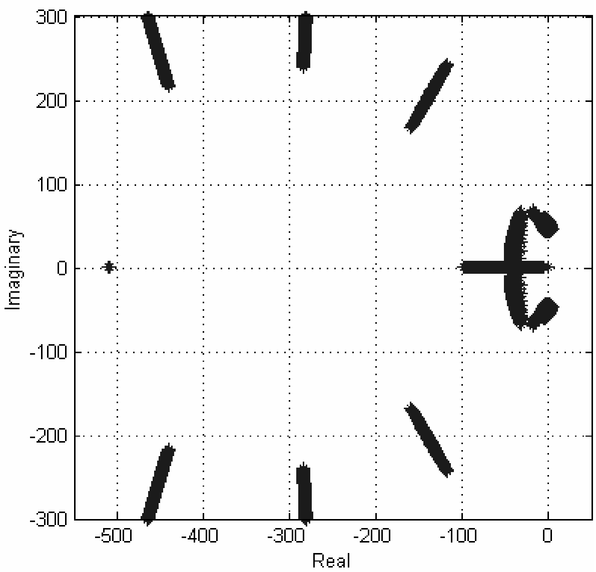


**Fig. 11:** *Effect of varying compensator bode gain (100-250) and load mass (50-500 lb) - $9^{th}$ order controller with critical frequency range between 6.5 Hz and 10 Hz depending on load mass*

## 5 Stability Boundary in Parameter Space

The control studies, as discussed in the previous section, for the two feedback control structures – a PD controller and a ninth-order linear controller – provide insight into the effect of various parameters on the bifurcation stability of the servo-valve actuator system. However, to effectively capture the nonlinear stability behavior due to change in the system parameters, it is essential to map the stability boundary in the parameter space. The stability boundary can be generated for two-dimensional grids on the parameter space. These results are also experimentally verified. During any such experimental verification, a parameter set for which the system is stable is chosen as a starting point. This starting point results in a constant velocity operation of the load mass in closed loop. The parameter is then varied in a particular direction on the selected two-dimensional parameter space until the loss of stability occurs. For all the cases presented in this paper, the loss of stability was due to Hopf bifurcation. Experimentally, Hopf bifurcation is manifested as emergence of limit cycle oscillations in the position of the electro-hydraulic cylinder, which in turn leads to large pressure oscillations in the system. In practical situations, these large pressure oscillations are detrimental to the system operation and performance.

The stability boundary for the PD controlled case is shown in Fig. 12 on the parameter space of the proportional gain and the derivative gain for controller. Experimental results agree with the numerical observations. Some deviation between the experimental and numerical results is attributed to identifying the limit cycle oscillations in the pressure signal data above the system noise level of 0.034 MPa (5 psi). Stability boundary in the space of load mass and proportional gain for the PD controller case is shown in Fig. 13. For the ninth-order linear controller case, the stability boundary is generated in the space of load mass and the Bode gain of the compensator (Fig. 14). The level cuts of changing the operating condition (constant velocity of system) is also depicted in Fig. 14. It is clearly visible that as the constant velocity is increased the stable region in the parameter space shrinks. This behavior is attributed to the increasing nonlinear behavior of the system as the constant velocity of operation is increased. The experimental result is in agreement with the numerical findings as shown in Fig. 14.

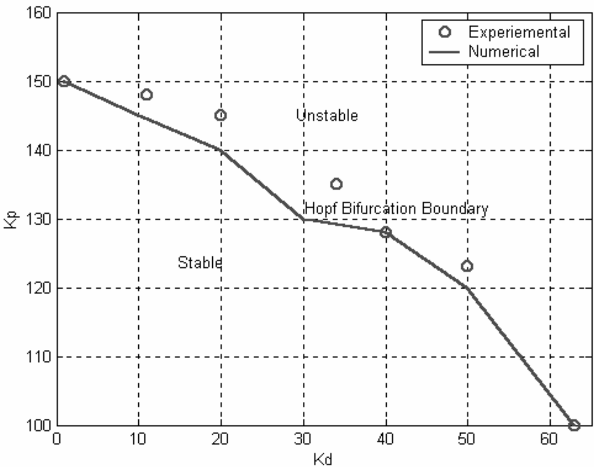


**Fig. 12:** *Stability boundary in two-dimensional parameter space ($K_p$, $K_d$) for load mass=370lb - experimental and numerical result –PD control*

In summary, the effect of various parameters on the stability boundary of servo-hydraulic systems has been demonstrated. The effect of two control structures on the stability has also been investigated. These investigations have been conducted by developing stability boundaries in two-dimensional parameter spaces. Further, it is shown that by designing a linear controller it is possible to extend the stability boundary and hence increase the stable region of the system. Increase in the order of the linear controller is demonstrated to have the potential to increase (expand) the stable region of the parameter space. This is clearly visible from the Fig. 15 which shows the stability boundary in the parameter space of Bode gain and load mass for the two control structures. It is shown that the ninth-order controller results in a larger stable region as compared to the PD controller for equivalent operating conditions. Thus appropriate design and selection of control structures can result in an increased margin. This results in an increased robustness to bifurcation stability.

## 6 Conclusions

In this work a detailed experimental investigation is carried out to develop a reduced-order model of an experimental servo-valve actuator system. Based on this reduced model, bifurcation studies are conducted and stability boundaries are generated for different control structures. These results are verified by the experimental parametric space investigations. It is shown that the loss of stability due to Hopf bifurcation is the most common in such systems. Also, the effect of two feedback control structures – PD control and a ninth order linear control on the stability boundary is studied. It is shown that a higher-order linear controller can increase the overall relative stability of the nonlinear closed loop system when compared to the PD controller. The higher-order control structure provides greater flexibility in the design of the controller. It is thus demonstrated that robustness to bifurcation stability can be extended by utilizing an appropriate control structure.

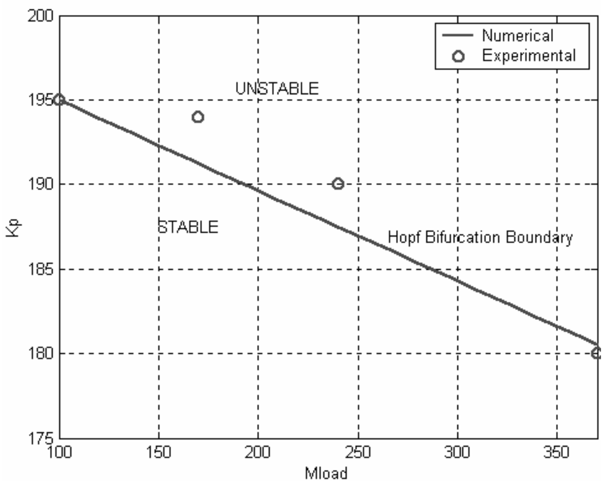


**Fig. 13:** *Stability boundary in two-dimensional parameter space ($M_{load}$, $K_p$) for constant velocity =0.2 in/sec and $K_d$=0.1- experimental and numerical result- PD control*

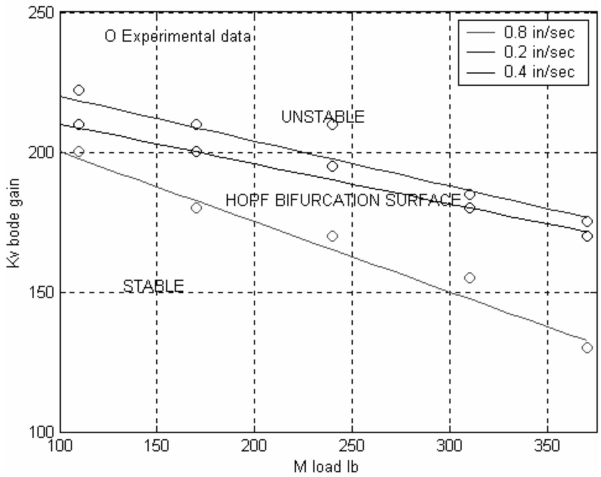


**Fig. 14:** *Bifurcation stability boundary in the 2-dimensional parameter space of load mass and Bode gain of the 9th order controller. Level cuts of constant velocity solution are shown. Experimental data matches closely with the numerical result*

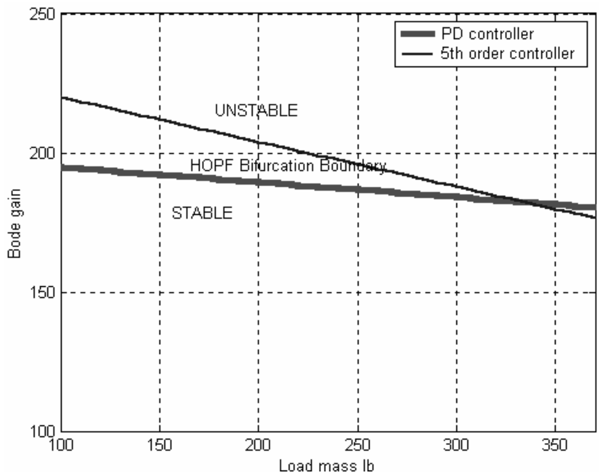


**Fig. 15:** *A comparison of the two controllers – PD and ninth-order for a constant velocity case (0.2 in/sec)*

## Nomenclature

| | |
|---|---|
| $V$ | Voltage input to servo-valve |
| $q$ | Flow |
| $\Delta p$ | Pressure differential |
| $k_{\text{valve}}$ | Valve flow constant |
| $x_{\text{valve}}$ | Valve spool position |
| $D_{\text{n}}$ | Pipe-line dissipation parameter |
| $Z_{\text{o}}$ | Pipe-line impedance constant |
| $\beta_e$ | Effective bulk modulus |
| $\rho_{\text{o}}$ | Density |
| $\nu$ | Kinematic viscosity |
| $m_{\text{load}}$ | Load mass |
| $c_{\text{load}}$ | Load damping constant |
| $k_{\text{load}}$ | Load stiffness |
| $P_{\text{a}}$ | Pressure associated with volume a |
| $A_{\text{cylinder}}$ | Cross section area of cylinder |
| $\alpha$ | Natural frequency modification factor for pipe-line dynamics |
| $\beta$ | Damping modification factor for pipe-line dynamics |

## Acknowledgement

The authors wish to acknowledge the financial support provided by the NSF (grant number CMS-9978704). The authors would also like to thank the anonymous reviewers for their comments and suggestions.

## References

**Alleyne, A.** and **Liu, R.** 1999. On the limitations of force tracking control for hydraulic servosystems. *Journal of Dynamic Systems, Measurement and Control, Transactions of the ASME*, vol. 121, no. 2, pp.122-137.

**Burton, R. T.** 1975. *Analytical and experimental prediction of limit cycle oscillations in an inertially loaded hydraulic control valve*. Ph.D. University of Saskatchewan,

**Blackburn, J. F., Reethof, G.**, and **Shearer, J. L.** 1960. *Fluid Power Control* Massachusetts. The MIT Press.

**Cox, C. S.** and **French, I. G.** 1986. Limit cycle prediction conditions for a class of hydraulic control systems. *Journal of Dynamic Systems, Measurement and Control, Transactions of the ASME*, vol. 108, pp. 17-23.

**D'azzo, J. D.** and **Houpis, C.H**. 1966. *Feedback control systems analysis and synthesi*, McGraw-Hill.

**Foster, K.** and **Kulkarni, M. M.** 1968. Steady amplitude, self excited oscillations of hydraulic spool valves. *Journal of Mechanical Engineering Science*, vol. 10, no. 4, pp. 306-317.

**Fuerst, D., Hahn, H.**, and **Hecker, E.** 1997. Mathematical modeling and parameter identification of a planar servo-pneumatic test facility. Part I: Mathematical modeling and computer simulation. *Nonlinear Dynamics*, vol. 14, no. 3, pp. 249-268.

**Guckenheimer, J.** and **Holmes, P.** 1983. *Nonlinear oscillations, dynamical systems, and bifurcation of vector fields*. Springer.

**Jordan, D.W.**, and **Smith, P.** 1999. *Nonlinear Ordinary Differential Equations: An Introduction to Dynamical Systems*. Third Edition, New York: Oxford Univ. Press.

**Kowta, S.** 2003. *Robust stability analysis of servo-hydraulic system in parameter space*. M.S. Thesis, University of Cincinnati, Cincinnati, Ohio.

**Kremer, G. G.** and **Thomson, D.F.** 1998. A bifurcation-based procedure for designing and analyzing robustly stable nonlinear hydraulic servo systems. *Proc. of Institution of Mechanical Engineers*, vol. 212, pp. 383-393.

**Krutz, J.E.** 2001. Design *of hydraulic actuator test stand for nonlinear analysis of hydraulic test stand*. Master's thesis, University of Cincinnati, Cincinnati, Ohio.

**Lewis, E. E.** and **Stern, H.** 1962. *Design of Hydraulic Control Systems.* McGraw Hill Book Co.

**Maccari, A.** 2000. Saddle-node bifurcations of cycles in a relief valve. *Nonlinear Dynamics*, vol. 22, no. 3, pp.221-231.

**McCloy, D.** and **Matrin, H.R.** 1980. *Control of Fluid Power.* John Wiley and Sons.

**Merritt, H. E.** 1967. *Hydraulic Control Systems.* John Wiley and Sons.

**Scheidl, R.** and **Manhartsgruber, B.** 1998. On the dynamic behavior of servo-hydraulic drives. *Nonlinear Dynamics*, vol. 17, pp. 247-268.

**Seydel R.** 1994. *Practical bifurcation and stability analysis: from equilibrium to chaos*. NY. Springer-Verlag.

**Shukla, A.** and **Thompson, D.F.** 2001. Bifurcation stability of servo-hydraulic systems. *Proc. of American Controls Conference*, pp. 3943-3948. Arlington, Virginia.

**Shukla, A.** and **Thompson, D.F.** 2002. Control of Bifurcations in Multidimensional Parameter Space for Servo-Hydraulic Systems. *Proc. of the 2002 American Control Conf.*. Anchorage, Alaska.

**Strogatz, S. H.** 2000**.** *Nonlinear Dynamics and Chaos***.** Preseus Publishing**.** Cambridge, MA.

**Van Schothorst, G.** 1997. *Modelling of Long-stroke Hydraulic Servo-systems for Flight-simulator Motion Control and System Design*. PhD Thesis. Delft University of Technology. Netherlands.

**Venkatasubramainian, V.**, **Schattler, H.**, and **Zaborszky, J.** 1995. Dynamics of large constrained nonlinear systems - a taxonomy theory. *Proc. of IEEE*, vol. 83, no. 11, pp. 178-191.

**Viall, E. N.** and **Zhang, Q.** 2000. Spool valve discharge coefficient determination. *Proc. of the 2002 American Control Conf., pp.491-495.*

**Viersma, T. J.** 1980. *Analysis, synthesis and design of hydraulic servosystems and pipelines*. NY. Elsevier.

**Watton, J.** 1988. Modelling of electrohydraulic systems with transmission lines using modal appoximations. *Proc***.** *of the IMechE*. vol. 202, no. B3, pp 153-163.

**Wiggins, S.** 1990. *Introduction to Applied Nonlinear Dynamical Systems and Chaos.* Springer.

**Yang W.C.** and **Tobler W.E.** 1991. Dissipative model approximation of fluid transmission lines using linear friction models. *Trans. Of ASME Journal of Dynamic Systems, Measurement and Control*, vol. 113, no. 1, pp. 152-162.

**Yau, Chin-Horng**, **Bajaj**, **Anil K.**, **Nwokah**, **Osita D. I.** 1992. Active control of chaotic vibration in a constrained flexible pipe conveying fluid. *American Society of Mechanical Engineers, Applied Mechanics Division, AMD*, vol. 152, pp. 93-108.

**Amit Shukla**
is an Assistant Professor at Miami University in the Department of Mechanical and Manufacturing Engineering. He received the M.S. and Ph.D. in mechanical engineering from University of Cincinnati in 1998 and 2002, respectively. His research interests include stability analysis and control of nonlinear systems.

**David F. Thompson**
is an Associate Professor at University of Cincinnati in the Department of Mechanical, Industrial and Nuclear Engineering. He received the M.S. degree from University of Michigan, Ann Arbor, in 1984 and the Ph.D. degree from Purdue University in 1990. His research interests include robust control design, nonlinear dynamics and optimal design with applications to transportation, propulsion, and power machinery.